Wireless Device Identification Based on Radio Frequency Fingerprint Features

Yun Lin[1], Jicheng Jia[1], Sen Wang[1], Bin Ge[2], Shiwen Mao[3]
[1]*College of Information and Communication Engineering, Harbin Engineering University, Harbin, 150001, P. R. China*
[2]*School of Mathematical Sciences, Harbin Engineering University, Harbin, 150001, P. R. China*
[3]*Department of Electrical and Computer Engineering, Auburn University Auburn, AL, 36849-5201, U.S.A.*
Email: linyun, jiajicheng, wangsen, gebin791025@hrbeu.edu.cn, and samo@ieee.org

***Abstract*—With the development of the Internet of Things (IoT) technology and the rapid deployment of 5G wireless, more and more radiation devices are appearing in the increasingly complex electromagnetic environment. To be able to manage these devices in a unified manner, accurate identification of the devices has become a top priority. Specific emitter identification (SEI) is to effectively solve this problem. In this paper, both power spectral density (PSD) and fractional Fourier transform (FrFT) methods are used to extract the characteristics of transient signals. The characteristics of steady-state signals are analyzed by the bispectrum method. The SEI system model in this paper is constructed based on these techniques. Our experiments results show that when the SNR is 16dB, the SEI system can achieve a recognition accuracy of over 97% by exploiting the characteristics of the transient signal. Since the characteristics of the steady-state signal can better suppress noise, the SEI system can achieve a nearly 90% classification recognition accuracy under extremely low SNR.**

***Index Terms*—Wireless device identification, Radio frequency fingerprint, Power spectral density, Fractional Fourier transform, Bispectrum**

I. Introduction

The rapid developments of the IoT and 5G wireless have resulted in more and more wireless devices being linked to each other, which brings about a series of regulatory and security problems. The SEI technology is proposed for identity authentication and device supervision of wireless devices [1]–[3], which can effectively solve the security and privacy issues and increase the security of the IoT. Therefore, accurate identification of radiation source devices of the same type has become a critical problem that should be addressed for communication security and privacy.

The SEI is a process of distinguishing individual transmitters by comparing RF fingerprints (RFFs) in received signals. These radio frequency (RF) fingerprints are the features of hardware devices that are inherent to the analog components in the transmitter and are independent of the information content. SEI is becoming more and more important, especially in cognitive radio and ad hoc networks [4]–[8]. Because the RFF of the equipment represents unique characteristics that are very difficult to tamper with and forge, it has a high potential for applying SEI for physical layer security, equipment identification, and certification [9].

For a common SEI system, the process of extracting the RFF and performing device identification is shown in Fig. 1.

In general, the SEI technology can be divided into two broad categories based on the signals it targets, namely the method of applying transient signals and that of applying steady-state signals. Transient signals which the power of the signal is increasing often contain a wealth of transmitter hardware features that provide a large number of RFFs for SEI, for example, based on variational mode decomposition and spectral features (VMD-SF) for transmitter identification [10]. It can also apply Hilbert transform to extract RFF and use SVM for classification, achieving a 90% recognition rate [11]. The disadvantage is that the duration is usually short, especially in the case of non-cooperative communications. After obtaining the RF signal of a transmitter, how to accurately intercept the transient signal segment becomes a problem that has to be addressed. Compared with transient signals, steady-state signals which the power of the signal is retention have a longer duration and stable power, which is more suitable for detection and feature extraction. The usual method can perform transform domain analysis, such as using the 3D-Hilbert spectrum and multi-scale segmentation features, which can achieve a nearly 90% recognition rate at low SNR [12]. Or the method could be an Information Data Estimation-based Stacking Algorithm (IDES) for DSSS systems. When the received signal SNR is -15 dB and the extended sequence length is 1023, it can achieve a 98% recognition rate [13]. Recently, there are some SEI methods based on statistical learning and deep learning. For example, using deep learning methods to detect physical-layer attributes to identify cognitive radios, a 92.29% recognition accuracy has been achieved with seven 2.4 GHz commercial ZigBee devices [14]. There are also hybrid approaches that integrate these two methods, such as the use of bispectrum as an RFF feature and then using a convolutional neural network (CNN) for SEI [15]. The latest SEI scheme first performs HHT and then uses the depth residual network to visually process the transformed graph, which finally achieves a recognition rate of nearly 98% [16].

The research on the RFF-based SEI technology is attracting more and more attention. The method has been proven to be effective and can be applied to fields such as security certification. Compared with other methods, the RFF utilized in SEI has the advantage of being unable to replicate. Therefore, this paper presents an in-depth study of the essential characteristics of RF signals and proposes three methods of

978-1-7281-5089-5/20/$31.00 ©2020 IEEE

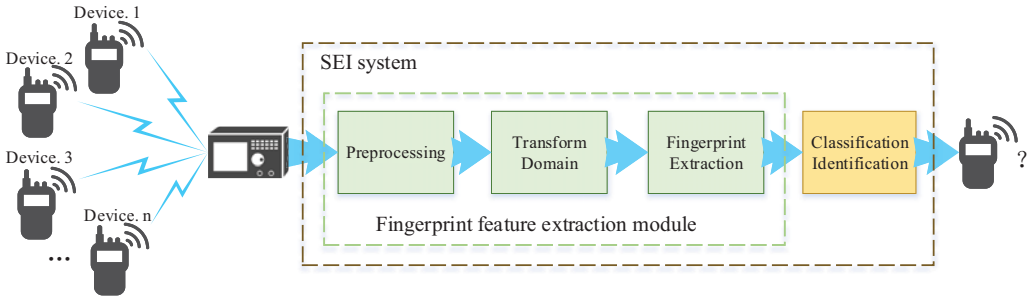

Fig. 1. The flow chart of device identification using SEI.

RFF extraction. In this paper, both the transient and steady-state signal segments of the RF signals are studied. The PSD method in frequency domain analysis and the FrFT method in time-frequency analysis are used to analyze the transient signals. The SEI method based on the steady-state signal is analyzed by the line integral bispectrum method. The final result shows that the SEI method of this paper can achieve nearly 100% transient signal recognition rate; and more than 90% of steady-state signal recognition rate.

The rest of this paper is organized as follows. Section II will introduce the RFF generation mechanism and the related theoretical basis applied in this paper. Section III will introduce the system model of SEI. The experiment and simulation results and analysis will be introduced in Section IV. Finally, Section V summarizes this paper.

II. Preltminaries

A. RF Fingerprint Generation Mechanism

The RFF of the communication radiation source refers to a series of feature sets extracted from the received signal by a feature extraction method, which includes the unique features of the device. The RFF features can be used to distinguish different radiation source devices. Fig. 2 shows the block diagram of a typical communication radiation source structure.

After the baseband digital signal passes through the DSP and DAC modules, it becomes an analog signal. And this analog signal is next processed by the analog circuits such as filtering, frequency conversion, and amplification. Finally, the source device transmits signals through the antenna. This part of the hardware circuit is the main cause of the RFF. Even with the same hardware circuit design implemented with the same type of electronic components, the RFFs of different devices are still different, due to different manufacturing process tolerances and device drift tolerances. The tolerance of the manufacturing process is relevant to the specific material and manufacturing process of the electronic components. The electrical parameter of the components usually has a certain deviation from the nominal value. Besides, the drift tolerance refers to electrical parameter changes caused by the aging of the component due to prolonged operation in the circuit. Furthermore, the voltage of power supply, operating time, temperature, humidity, board material, and layout traces also form unique features that affect the transmitted RF signal. In summary, all the different features described above together generate the RFF feature for performing classification and identification of the radiation source device.

Besides, the receiver device usually has a certain impact on emitter identification. Therefore, the SEI needs to use high precision and consistent equipment to receive the emitter signal, which can reduce the impact of the receiver device and make the recognition result more accurate.

B. Received RF Signal

Fig. 3 shows the typical waveform of a power-on signal, which consists of two segments. The transient signal refers to a signal segment of short duration, which is the irrelevant transmitted signal generated by the radiation source device at the moment of switching on or off. Since it is only related to the hardware circuit of the device and contains the fine feature information of the rich radiation source device, the transient signal is a suitable signal for classification and identification of the radiation source.

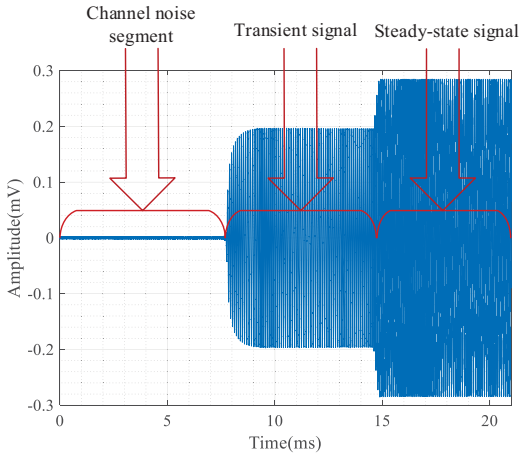

Fig. 3. Waveform of a typical power-on signal.

The steady-state signal refers to the signal segment of the transmitter RF signal that operates stably at rated power. The steady-state signal has a longer duration and is easier to acquire than the transient signal. However, the subtle features of the device are often hidden in the main component of the signal, which makes the feature extraction more difficult, as compared to that using the transient signal.

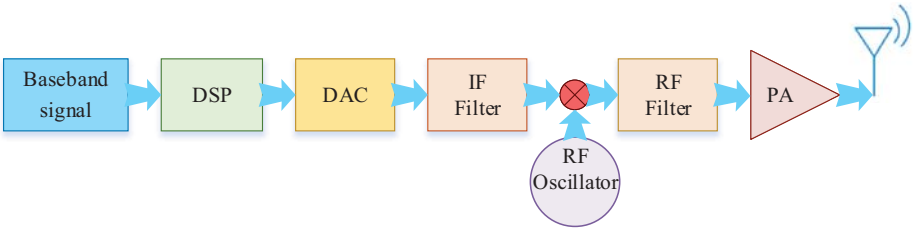

Fig. 2. Block diagram of a typical communication radiation source structure.

C. PSD-Based RFF Extraction

In general, time-domain features are greatly affected by signals, resulting in unsatisfactory recognition results. Power Spectral Density (PSD) is a good method of frequency domain analysis, which can be used to extract the fingerprint characteristics of the radiation source. Given a time-domain signal sample series $x(n), n = 1, 2, \cdots, N$, the PSD expression of the signal can be obtained by the discrete Fourier transform (DFT) as

$$X(k) = \frac{1}{N}\sum_{n=1}^{N} x(n)e^{-j\Phi(N,n,k)} \tag{1}$$

$$\Phi(N, n, k) = \left(\frac{2\pi}{N}\right)(n-1)(k-1) \tag{2}$$

To reduce the error due to receiver bias, the normalized PSD expression here is calculated from the given estimated power spectral density as

$$P_x = \frac{1}{N}\sum_{n=1}^{N} x(n)x^*(n) \tag{3}$$

where x^* represents the conjugate expression of the signal. The combined (1) and (2) can be used to obtain a normalized PSD expression as

$$\bar{p}(k) = \frac{1}{P_x}|X(k)|^2 \tag{4}$$

Once the PSD of signals is obtained using (4) , then we can apply PSD to extract RFF features for device identification.

D. FrFT-Based RFF Extraction

PSD analyzes only in the frequency domain, losing information such as the instantaneous frequency and phase of the signal. Fractional Fourier Transform (FrFT) is a powerful tool for time-frequency domain analysis. It has great advantages in analyzing non-stationary signals. FrFT is a generalized form of Fourier Transform. FrFT can be regarded as an FT that rotates counterclockwise at any angle α in the time-frequency plane. The calculation process of its discrete form is as follows.

The FrFT is defined as:

$$F_p = DK_pJ \tag{5}$$

where D and J are twice the matrices of interpolation and decimation operations, respectively, and K_p is the transformation kernel matrix of discrete FrFT, given by:

$$K_p = \sqrt{\frac{1-\mathrm{j}\cot\alpha}{8N}}\exp\left(\frac{j\pi(\cot\alpha)m^2}{4N} - \frac{j\pi(\csc\alpha)mn}{4N} + \frac{j\pi(\cot\alpha)n^2}{4N}\right) \quad |m|, |n| \le N \tag{6}$$

Dimension normalized discretization FrFT is defined as:

$$X_p(u) = \sqrt{\frac{1-\mathrm{j}\cot\alpha}{2\pi}}\exp\left[\mathrm{j}\pi\cot(\alpha)u^2\right] \times \int_{-\infty}^{\infty} x(t)\exp\left[\mathrm{j}\pi\cot(\alpha)t^2\right]\exp\left[\mathrm{j}\pi\cot(\alpha)tu\right]\mathrm{d}t \tag{7}$$

Among them, $\alpha = p\pi/2$ is the angle of FrFT rotating counterclockwise on the time-frequency plane, which is a fractional-order with a value in $(0, 1)$.

E. Bispectrum-Based RFF Extraction

The bispectral transform analysis of the signal has the advantages of phase retention, scale variability, and time shift-invariance [17]. These advantages ensure that the radiated source signal will not lose too much useful information after being transformed, which is highly beneficial to classification and identification of the radiation source equipment. Moreover, theoretically, high-order spectral analysis can immunize Gaussian noise. Just because the bispectrum transform is not conducive to classification and recognition, it will consume a lot of resources for recognizing two-dimensional images. Therefore, the two-dimensional image will firstly be integrated into a one-dimensional function value by the method of line integral bispectrum.

There are four types of well-integrated bispectrum algorithms: axial integral bispectrum (AIB), circumferential integral bispectrum (CIB), radial integral bispectrum (RIB), and rectangular integral bispectrum (SIB). First, the bispectrum of signal $x(t)$ can be expressed as follows.

$$B_x(\omega_1, \omega_2) = \sum_{\tau_1=-\infty}^{\infty}\sum_{\tau_2=-\infty}^{\infty} c_{3x}(\tau_1, \tau_2)e^{-j(\omega_1\tau_1+\omega_2\tau_2)} \tag{8}$$

where:

$$C_{3x}(\tau_1, \tau_2) = \int_{-\infty}^{+\infty} x^*(t)x(t+\tau_1)x(t+\tau_2)\,\mathrm{d}t = \mathrm{E}\left\{x^*(t)x(t+\tau_1)x(t+\tau_2)\right\} \tag{9}$$

is the third-order correlation function of the signal. We then show how to compute surround line integral double spectrum in the remainder of this section.

a) AIB: The AIB algorithm mainly integrates the bispectrum along the ω_1 or ω_2 axis, and assumes that the bispectrum is $B(\omega_1, \omega_2)$ (see (8) for signal $x(t)$).

$$\begin{aligned} AIB(\omega) &= \frac{1}{2\pi}\int_{-\infty}^{\infty} B(\omega_1, \omega_2)\, d\omega_2 \\ &= \frac{1}{2\pi}\int_{-\infty}^{\infty} B(\omega_1, \omega_2)\, d\omega_1 \end{aligned} \tag{10}$$

It can be seen from the Fourier transform projection that the AIB can be regarded as the Fourier transform of the axial section of the third-order correlation function of the signal.

b) CIB: The integration path of the CIB algorithm is a series of concentric circles with the origin as the center of the circle. The bispectral values on the concentric circles are discretely summed up to obtain the CIB value, which is specifically defined as:

$$CIB(\alpha) = \int B_p(\alpha, \theta)\, d\theta \tag{11}$$

where $B_p(\alpha, \theta)$ is the polar coordinate representation of the bispectral estimate. CIB retains some phase information which is scale invariance, but the integral path is more complex than other integration methods. In actual operations, the loss of plane points and repeated calculations will be caused by uneven sampling.

c) RIB: RIB is obtained by discrete summation of bispectral values on a straight path through the origin in a bispectral plane. According to the integral bispectrum phase, the RIB is defined as:

$$RIB(\alpha) = \arctan\left(\frac{I_i(\alpha)}{I_r(\alpha)}\right) \tag{12}$$

where $I(\alpha) = I_r(\alpha) + jI_i(\alpha) = \int_{0+}^{1/(1+\alpha)} B(f_1, \alpha f_1)\, df_1$, and $B(f_1, \alpha f_1)$ is the bispectral value of the signal. It mainly computes the discrete summation of the linear path passing through the origin in the bispectral plane, while the phase information of the bispectrum are retained.

d) SIB: SIB accumulates each side of a series of rectangles centered on the bispectral origin as the integral path, and the SIB integral is calculated as:

$$SIB(\omega) = \oint_{S_l} B(\omega_1, \omega_2)\, d\omega_1 d\omega_2 \tag{13}$$

where S_l represents the integral path of the rectangular integral bispectrum. From the calculation process, the SIB can make full use of the feature information in the bispectral plane without missing or repeating calculation of the bispectral points.

After calculating the bispectrum of the signal and obtain a set of one-dimensional vectors through the bispectral integration, we can use the resulting one-dimensional vector as the RFF feature of the devices.

III. System Framework

A. System Structure

The SEI system is constructed as shown in Fig. 4, where the PSD-based method is used as an example.

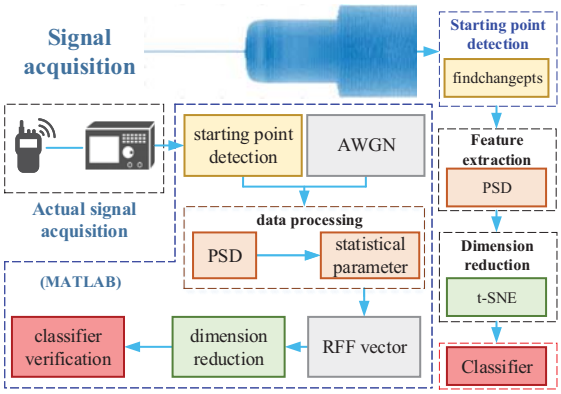

Fig. 4. SEI system block diagram.

After collecting the intercom signal (e.g., using an oscilloscope), we intercept useful signal segments and superimpose Gaussian noise for a target SNR level. Then we extract the RFF vector and use t-SNE to reduce the dimension of the vector [18]. Finally, the RFF is fed into an SVM model to obtain the classification recognition results. The Classification recognition rate is the performance metric for verifying the effectiveness of the feature extraction method.

B. RFF Extraction Algorithm

The flow of the proposed RFF extraction algorithm is shown in Algorithm 1 (taking the PSD-based method as an example).

Algorithm 1: PSD-based RFF Extraction Algorithm

Data: RF signals and device labels;
Input: RF transient signal;
Output: RFF vector: $sta\_feature$;

Import the RF transient signal, initialize the sample number m, label $class\_num$, segment number N, and the feature vector $sta\_feature(m,\ 3*N+1)$;
for $m\_range = 1, 2, 3, ..., m$ **do**
  Calculate the PSD for each sample;
  Divide the sample PSD into segments;
  for $i = 1, 2, 3, ..., N$ **do**
    Calculate variance σ^2, skewness γ, and kurtosis κ of the i-th segment of the sample PSD, then obtain $F_i^x = [\sigma_x^2, \gamma_x, \kappa_x]$;
    $sta\_feature(m\_range,\ 3*i) = F_i^x = [\sigma_x^2, \gamma_x, \kappa_x]$;
  end
end
$sta\_feature(\ :\ ,\ \text{end}) = class\_num$;
return $sta\_feature$;

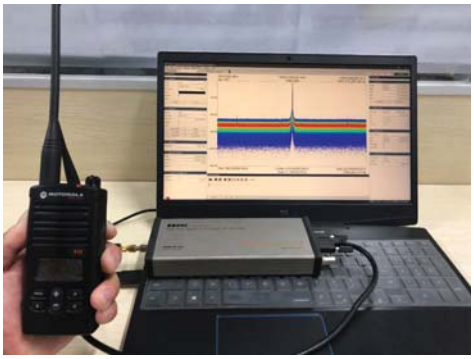

Fig. 5. Illustration of how the walkie-talkie signal dataset is collected in our experiment.

TABLE I
MEASURED SIGNAL PARAMETERS

Acquisition parameter	Parameter value
Modulation	FM
Frequency	410 MHz
Sampling rate	24 MHz
Sampling points	350000

C. The Dataset

Without loss of generality, this paper uses walkie-talkie equipment as an example to carry out simulation data acquisition and simulation verification of the proposed algorithm. The scenario of signal acquisition is shown in Fig. 5, where the BB60C walkie-talkie device is used. The equipment to be identified is selected from 10 walkie-talkie handsets with the same model, i.e., Motorola A12. The specific device acquisition parameters are shown in Table I.

During the experiment, 50 signal samples are collected for each walkie-talkie handset, and a total of 500 signal samples are obtained. To verify the generalization performance of the algorithm, a cross-validation method is used to divide the training and test datasets, wherein the ratio of training to test samples is 3:2.

IV. RESULTS AND DISCUSSIONS

A. Simulation Results

The SEI simulation is performed using the walkie-talkie dataset. The system architecture is shown in Fig. 4. PSD and FrFT methods are used with transient signals for RFF extraction, and the four surrounding line integral bispectral methods are used with steady-state signals. The RFF vector is reduced to 8 dimensions by using t-SNE, and the SVM is used for device identification classification.

The ability of the SEI method to identify the source walkie-talkie handset under noise is verified by adding different levels of noises to the original signal.

Fig. 6 presents the SEI recognition results with transient signals. It can be seen from Fig. 6 that the two SEI methods with transient signals can achieve a recognition rate of higher than 90%, when the SNR is greater than 10 dB. The PSD method can achieve a recognition rate of over 90% when the SNR is increased to 2 dB and its recognition rate stabilizes around 94% when the SNR is further increased. FrFT is less

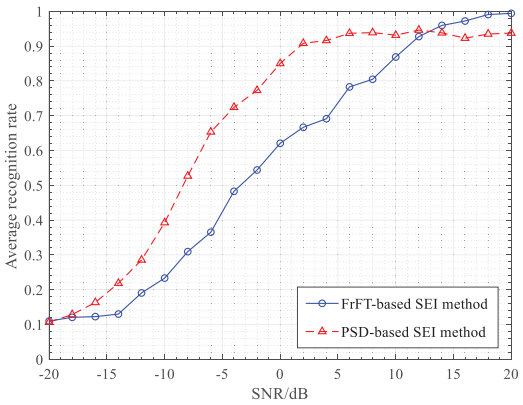

Fig. 6. SEI recognition results using transient signals.

resistant to noise, but it starts to outperform the PSD method when the SNR is higher than 14dB, and its recognition rate converges to 100% when the SNR is higher than 20 dB.

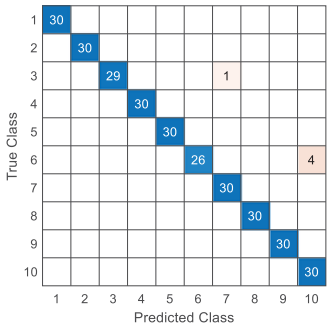

Fig. 7. FrFT-based SEI recognition confusion matrix (SNR=10dB).

Fig. 7 plot the recognition confusion matrix of the SEI based on the FrFT method using transient signal, when the SNR is 10dB. It can be seen that the recognition effect is pretty good, but Device 6 could be easily misclassified as device 10.

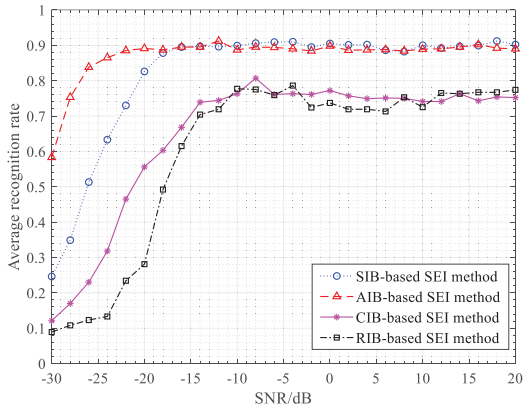

Fig. 8. SEI recognition results using steady-state signals.

Fig. 8 presents the recognition results of the SEI methods using steady-state signals. It can be seen from Fig. 8 that when the SNR is higher than -18dB, the overall average recognition of the AIB and SIB based RFF extraction algorithms becomes optimal, which is around 90%. The RFF extraction algorithms based on CIB and RIB is slightly worse. When SNR is greater than -10dB, a stable recognition result is reached by these two algorithms which are around 75%.

Fig. 9 plots the identification confusion matrix for the SEI based on the AIB method using steady-state signal, when

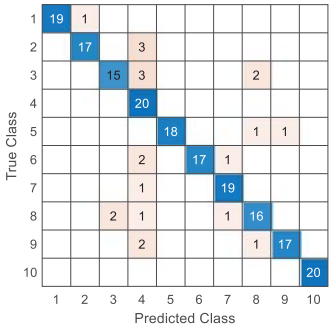

Fig. 9. AIB-based SEI recognition confusion matrix (SNR=10dB).

the SNR is also 10dB. We find that Device 1, 4, 7, and 10 can be well distinguished. Among them, the recognition rate of Device 3 is the worst. Besides, this method could easily misclassify a device as Device 4, and the misclassification rate of this case is 37.5%.

B. Discussions

The experimental results show that the transient signal contains rich transmitter characteristics. And because the transient signal does not contain modulation signal interference, the RFF vector extracted from it can be a good representation of the radiation source device. That is, the SEI method using transient signal has a higher recognition rate at high SNR, but the method is susceptible to noise and its recognition rate will degrade quickly at low SNR.

On the other hand, due to the presence of modulated signal, most of the features in the steady-state signal are submerged, thus the recognition rate of this method is lower. But because of its relatively higher power, employing bispectrum analysis method, a recognition rate of about 90% can still be achieved even when the SNR is low. The SEI method using steady-state signal mitigates the problem of a decrease in the recognition rate in the presence of severe noise interference, but at the cost of a poor performance at the high SNR region.

V. Conclusion

This article focuses on SEI issues. To fully exploit the features of RF signals, we proposed PSD and FrFT based RFF feature extraction methods using transient signals, as well as bispectrum analysis based methods using steady-state signals. This proposed scheme used t-SNE for reducing the data dimension and incorporated SVM to classify devices. The experiment results showed that all three methods have reached a satisfactory performance. When the SNR is higher than 6dB, the recognition rate with transient signals is higher than 95%; when the SNR was higher than -20dB, the recognition rate using steady-state signals was higher than 90%. Therefore, the features extracted by the three methods accurately describe the difference between the radiation source signals and enable accurate device identification.

With the development of the SEI technology, future research could be focused on how to effectively and conveniently obtain identifiable signals. Besides, how to obtain better and more reliable identification result is also important under the influence of channel dynamics.

Acknowledgment

This work is supported by the National Natural Science Foundation of China (61771154) and the Fundamental Research Funds for the Central Universities (HEUCFG201830, GK2080260148). This research is also funded by the International Exchange Program of Harbin Engineering University for Innovation-oriented Talents Cultivation.

References

[1] B. Danev, D. Zanetti, and S. Capkun, "On physical-layer identification of wireless devices," *ACM Computing Surveys (CSUR)*, vol. 45, no. 1, pp. 1–29, 2012.

[2] L. Peng, A. Hu, J. Zhang, Y. Jiang, J. Yu, and Y. Yan, "Design of a hybrid rf fingerprint extraction and device classification scheme," *IEEE Internet of Things Journal*, vol. 6, no. 1, pp. 349–360, 2018.

[3] Y. A. Eldemerdash, O. A. Dobre, O. Üreten, and T. Yensen, "Identification of cellular networks for intelligent radio measurements," *IEEE Transactions on Instrumentation and Measurement*, vol. 66, no. 8, pp. 2204–2211, 2017.

[4] Z. Zhang, K. Long, and J. Wang, "Self-organization paradigms and optimization approaches for cognitive radio technologies: a survey," *IEEE Wireless Communications*, vol. 20, no. 2, pp. 36–42, 2013.

[5] Q. Xu, R. Zheng, W. Saad, and Z. Han, "Device fingerprinting in wireless networks: Challenges and opportunities," *IEEE Communications Surveys & Tutorials*, vol. 18, no. 1, pp. 94–104, 2015.

[6] O. A. Dobre, "Signal identification for emerging intelligent radios: Classical problems and new challenges," *IEEE Instrumentation & Measurement Magazine*, vol. 18, no. 2, pp. 11–18, 2015.

[7] Y. A. Eldemerdash, O. A. Dobre, and M. Öner, "Signal identification for multiple-antenna wireless systems: Achievements and challenges," *IEEE Communications Surveys & Tutorials*, vol. 18, no. 3, pp. 1524–1551, 2016.

[8] Z. Zhang, J. Chang, M. Chai, and N. Tang, "Specific emitter identification based on power amplifier.," *International Journal of Performability Engineering*, vol. 15, no. 3, 2019.

[9] Y. Chen, H. Wen, H. Song, S. Chen, F. Xie, Q. Yang, and L. Hu, "Lightweight one-time password authentication scheme based on radio-frequency fingerprinting," *IET Communications*, vol. 12, no. 12, p-p. 1477–1484, 2018.

[10] U. Satija, N. Trivedi, G. Biswal, and B. Ramkumar, "Specific emitter identification based on variational mode decomposition and spectral features in single hop and relaying scenarios," *IEEE Transactions on Information Forensics and Security*, vol. 14, no. 3, pp. 581–591, 2018.

[11] Z. Zhang, X. Guo, and Y. Lin, "Trust management method of d2d communication based on rf fingerprint identification," *IEEE Access*, vol. 6, pp. 66082–66087, 2018.

[12] Y. Lin, X. Zhu, Z. Zheng, Z. Dou, and R. Zhou, "The individual identification method of wireless device based on dimensionality reduction and machine learning," *The Journal of Supercomputing*, vol. 75, no. 6, pp. 3010–3027, 2019.

[13] Y. Xing, A. Hu, J. Zhang, L. Peng, and G. Li, "On radio frequency fingerprint identification for dsss systems in low snr scenarios," *IEEE Communications Letters*, vol. 22, no. 11, pp. 2326–2329, 2018.

[14] K. Merchant, S. Revay, G. Stantchev, and B. Nousain, "Deep learning for rf device fingerprinting in cognitive communication networks," *IEEE Journal of Selected Topics in Signal Processing*, vol. 12, no. 1, pp. 160–167, 2018.

[15] L. Ding, S. Wang, F. Wang, and W. Zhang, "Specific emitter identification via convolutional neural networks," *IEEE Communications Letters*, vol. 22, no. 12, pp. 2591–2594, 2018.

[16] Y. Pan, S. Yang, H. Peng, T. Li, and W. Wang, "Specific emitter identification based on deep residual networks," *IEEE Access*, vol. 7, pp. 54425–54434, 2019.

[17] C. L. Nikias and M. R. Raghuveer, "Bispectrum estimation: A digital signal processing framework," *Proceedings of the IEEE*, vol. 75, no. 7, pp. 869–891, 1987.

[18] A. Gisbrecht, A. Schulz, and B. Hammer, "Parametric nonlinear dimensionality reduction using kernel t-sne," *Neurocomputing*, vol. 147, pp. 71–82, 2015.